Chapter 1

Introduction and Background

1.1 Motivation

The AAAS (American Association for the Advancement of Science) Atlas of Population and Environment has stated that during the past 50 years, global consumption of commercial energy has risen more than fourfold, far outpacing the rise in population. In one way or another, energy comes from natural resources, whether it be fossil fuels such as coal and oil, living resources such as timber and biomass, nuclear fuel such as uranium, or renewable resources such as flowing water, wind or power from the sun. A generation ago, there was concern that fossil fuels would run out, plunging the world into an energy crisis. Today, the fear is that their continued use might destroy the global climate through carbon dioxide emission.

Energy is used to illuminate, heat and cool our living spaces, for cooking, manufacturing, transportation, and for myriad other purposes. About 29% of our total energy consumption is used for tranportation. Statistics from the U.S. Government, Energy Information Administration estimate that the total delivered energy consumption in the transportation sector as of this writing is 28.8 quadrillion Btu and it is projected to increase to 31.9 quadrillion Btu in 2030. A shift to cleaner, more-efficient sources of energy is vital.

Looking at nature for inspiration in engineering design, a major difference can be noted in the method of locomotion. Animals typically propel using unsteady dynamics producing vortex rings. Vortex rings have been shown in the wakes of fish such as mackerel (Borazjani and Sotiropoulos 2008), sunfish (Drucker and Lauder 1999), eels (Tytell and Lauder 2004) and other marine animals such as squid (Anderson and Grosenbaugh 2005) and jellyfish (Dabiri et al. 2005) to name a few. Using unsteady jet propulsion, aquatic animals have been shown to display high propulsive efficiencies. Fish (1998) has shown that dolphins can display propulsive efficiencies as high as 84% using certain swimming kinematics. The theoretical anaylysis of Weihs (1977) indicates that an unsteady jet with vortex ring formation can augment thrust and efficiency by nearly an order of magnitude compared to the steady jet propulsion system. It is essential to consider the role of vortex ring formation in increasing the propulsive performance of engineered systems.

1.2 Background

1.2.1 Pulsed Jets

When an organism or vehicle uses pulsed jet propulsion for locomotion, the jet created is highly unsteady and consists of bursts of fluid. A multiplicity of such bursts of fluid or pulses, is called a fully pulsed jet and can lead to a multiplicity of vortex rings in the jet wake. When the unsteady component is a small fraction of the mean jet velocity, this case is referred to as a forced jet. In the limit that the jet velocity returns to zero in between pulses, even for a finite amount of time, the jet is referred to as a fully pulsed jet. The literature on fully pulsed jets is not as abundant in comparison to the literature for forced jets.

Most of the literature on forced jets has focused on the dynamics of the mean and fluctuating velocities of the jet, on the enhancement of ambient fluid entrainment and mixing effects resulting from forcing. When a jet is used for thrust augmentation, or the mixing process, a large mass entrainment near the jet nozzle is desired. Research has also focused on the dynamics of coherent structures produced in the near jet region and the transition to turbulence, (Broze and Hussain 1994, 1996). Crow and Champagne (1971) were among the first to recognize the importance of orderly structures in turbulent jets. Work by Vermeulen et al. (1992) shows that entrainment can be enhanced by acoustic excitation of the jet flow.

Fully pulsed jets have been studied experimentally by Bremhorst and Hollist (1990), Bremhorst and Gehrke (2000) and Krueger (2005). Bremhorst and Hollist (1990) obtained velocity field measurements up to 100 jet diameters downstream from the nozzle. They noted that the ordered nature of the leading vortex produced by each pulse yielded a region of pulse-dominated flow that extended to 50 diameters downstream, and it was not until after this point that the centerline velocity decay and centerline turbulence intensities approached those expected for a steady jet. The Reynolds stresses were considerably larger for the fully pulsed jet than for a steady jet and were considered to be responsible for increased entrainment due to the vortex ring formed by each pulse. Bremhorst and Gehrke (2000) obtained measurements of Reynold stresses and energy budgets in the downstream region (distances greater than 50 diameters from the nozzle) of the jet for the application of modeling turbulence. Krueger (2005) investigated thrust augmentation in a fully pulsed jet as a function of dimensionless pulse size (L/D) and dimensionless frequency (Sr_L). Significant thrust augmentation was observed over the entire parameter range tested when compared to an equivalent steady jet with an identical mass flux. Augmentation appeared to be greatest at small values of L/D. In addition, Krueger noted that as Sr_L increases, the vorticity from preceding pulses is closer to the nozzle at the ejection of each pulse, requiring less fluid to be accelerated by the issuing pulse, therefore reducing nozzle exit overpressure.

1.2.2 Vortex Ring Formation

The concepts of vortex ring formation and issues related to the dynamics of laminar and turbulent vortex rings have been reviewed by Lim and Nickels (1995) and Shariff and Leonard (1992). Vortex rings are most commonly formed in a laboratory using piston-cylinder arrangements. They are generated by the motion of a piston pushing a column of fluid of length L through an orifice or nozzle of diameter D. As fluid is ejected this results in the separation of the boundary layer at the edge of the orifice or nozzle and subsequent spiral roll up. When a single burst of fluid is issued from a nozzle into a quiescent fluid, it is referred to as a starting jet. The evolution of the vortex ring size, position, and circulation have been studied experimentally by Didden (1979), Maxworthy

(1977) and Glezer (1988). In Didden (1979), the research provided insight on the role of internal and external boundary layers in the formation process and circulation of the vortex ring. Saffman (1978) and Pullin (1979) modeled the initial roll up process using similarity theory and obtained expressions for the vortex ring trajectory, circulation, and its vorticity distribution. Nitsche (1996) determined the properties of a vortex ring as a function of the piston motion and found that the initial ring diameter, core size and circulation are well predicted by planar similarity theory.

Most work regarding vortex ring formation ignores the roll up process of the vortex sheet. In most instances, the amount of each dynamic quantity (circulation, impulse, and energy) generated by the piston-cylinder is modeled using a slug flow model where the ejected fluid is seen as having a uniform velocity equal to the piston velocity and pressure equal to the ambient pressure. Glezer (1988) used this model to determine vortex ring impulse. Despite oversimplification, the slug flow model is still used in vortex ring research.

Work by Gharib et al. (1998) showed that the circulation, impulse, and energy of a vortex ring is dependent on stroke ratio. The maximum circulation that a vortex ring can attain during its formation is reached at a stroke ratio of approximately 4, which is referred to as the formation number. Krueger and Gharib (2003) investigated the impulse and thrust generated by starting jets for L/D ratios in the range of 2–8. He showed that a local maximum in average thrust exists for pulses near L/D values associated with vortex rings whose circulation had been maximized. This maximization was shown to be related to the nozzle exit overpressure generated during vortex ring formation. Work by Krueger et al. (2006) examined the formation number of vortex rings formed in uniform background coflow and Dabiri and Gharib (2004) in an imposed bulk counterflow.

The benefit of vortex ring formation for propulsion arises due to the entrainment of ambient fluid by the forming vortex ring (Auerbach 1991, Dabiri 2004, Olcay and Krueger 2008) in addition to the added mass of nonentrained fluid surrounding the vortex that must be accelerated with the vortex ring (Krueger and Gharib 2003). The schematic of a fully developed vortex ring on the left of figure 1.1 illustrates the two classes of ambient fluid accelerated by a starting jet. The ambient fluid entrained into the vortex ring as the shear layer from the nozzle boundary layer rolls up into a ring near the nozzle exit was first noted by Didden (1979). This effect is apparent by the dark bands in the vortex ring in the planar laser-induced fluorescence image in figure 1.1. The second benefit of vortex ring formation, the added mass effect, occurs as a portion of the fluid in front of the jet must be accelerated out of the way when the starting jet is initiated and ambient fluid must be brought behind the vortex ring to preserve continuity once the vortex begins moving downstream. This effect is illustrated on the left image in figure 1.1 and is represented by the outer dotted oval. The added mass effect is mathematically equivalent to the added mass carried with a solid body in potential flow and can be computed in terms of the velocity potential of the flow outside of the vortex (Dabiri 2006).

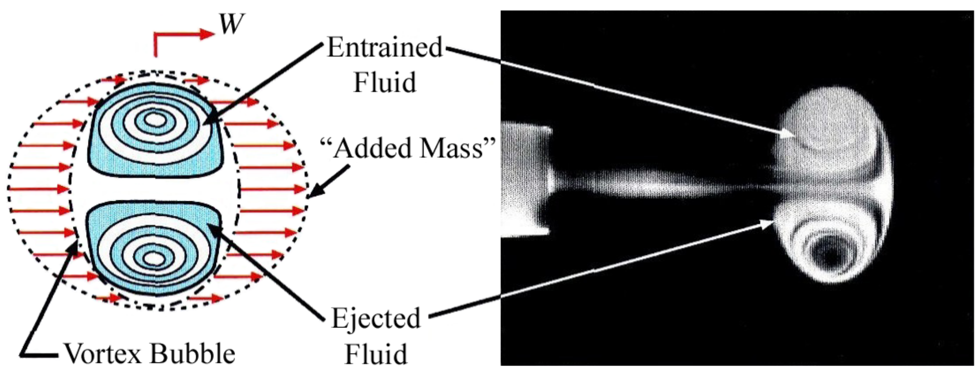

Figure 1.1. Illustration of the two classes of ambient fluid accelerated by a vortex ring. The image on the right is a PLIF flow visualization, Krueger (2001).

1.2.3 Bio-Mimetic and Bioinspired Devices

A rapidly growing area of interest in hydrodynamics and hydropropulsion is the application of strategies used by swimming animals in order to improve current propulsive technology. These efforts have largely involved mimicking the shape and kinematics of swimming animals in order to achieve there propulsive performance and are classified as bio-mimetic devices. In recent years, research in fluid flow mechanisms used by fish for propulsion and maneuvering has demonstrated the utility of bio-propulsion for undersea vehicles. Barrett et al. (1999) illustrated with his RoboTuna apparatus, that manipulation of the body of an undersea vehicle in a fishlike manner could significantly enhance energetic performance. Anderson and Chhabra (2002) designed and developed a vehicle that uses vorticity control propulsion and maneuvering, known as VCUUV (vorticity control unmanned undersea vehicle) to study the energetics and maneuvering performance of fish-swimming propulsion. VCUUV is a self-contained free-swimming research vehicle that follows the morphology and kinematics of yellowfin tuna. Others, (Tangorra et al. 2007) have been inspired by the coordinated motion of a fish fin and have embarked on research to develop a maneuvering propulsor for unmanned undersea vehicles that is based on the pectoral fin of the bluegill sunfish. Wilbur and collaborators (Ayers et al. 2001) have designed a lamprey-based undulatory vehicle that takes advantage of the animal's manuverablity and energetic efficiency as they produce a reduced-wake signature.

1.2.4 Metrics of Propulsive Performance

Aquatic animals differ from typical engineering systems in their use of unsteady flow for locomotion. Traditional definitions of propulsive efficiency used to model these behaviors have not taken unsteady effects into account and are typically based on steady flow through propellers or rocket motors. Measurements of aquatic animals based on these quasi-steady metrics have suggested propulsive efficiencies over 80% when utilizing certain swimming kinematics. However, the mechanical efficiency of muscle-actuated biological propulsion has been found to be much lower, typically less than 20%. When designing and implementing a biologically inspired propulsive device, it is important to take into account the overall efficiency (η_o) of the system defined as the product of the mechanical (η_{mech}) and propulsive efficiency (η_{prop}) (Hill and Peterson 1992).

$$\eta_o = \eta_{mech} \times \eta_{prop} \tag{1.1}$$

The η_{mech}, is a measure of the efficiency of converting the energy input into mechanical power to drive the propulsion mechanism. For shaft power devices, the mechanical efficiency is defined by

$$\eta_{th} = \frac{P_s}{P_{in}}, \tag{1.2}$$

where P_s is shaft power and P_{in} is the heat energy or power input. The η_{prop} is a measure of the performance of the propulsion system and is the ratio of useful work to the mechanical energy produced in the fluid. The mechanical energy is the increase in kinetic energy of the fluid per unit time. The useful work is the product of thrust, T, and the speed of the vehicle relative to the surrounding fluid, U. The propulsive efficiency can be written as

$$\eta_{prop} = \frac{T\,U}{\dot{m}\left[(U_j^2 - U^2)/2\right]}, \tag{1.3}$$

where $\dot{m}$ is the mass flow rate through the propulsion system and U_j is the speed of the jet flow. Using conservation of momentum, the thrust for a steady jet can be approximated as $T = \dot{m}(U_j - U)$. Making the following substitution into equation (1.3), the propulsive efficiency simplifies to

$$\eta_{prop} = \frac{2}{1 + U_j/U}. \tag{1.4}$$

This result is the ideal (i.e., steady, inviscid) efficiency for a propeller and is otherwise known as the Froude efficiency, Glauert (1935). As a consequence of the steady flow assumption, schemes to enhance propulsive efficiency have focused on manipulating the mean velocity profiles upstream and aft of the propulsor. These efforts have included the use of coaxial contrarotating propellers (Hadler 1969), propellers with vane wheels (Grim 1980, Blaurock 1990), ducted propellers (Stipa 1931, Sachs and Burnell 1962), pre- and post-swirl devices (Narita et al. 1981, Grothues-Spork 1988), and flow-smoothing devices (Glover 1987). These strategies typically provide increases in propulsive efficiency of only a few percent, with a few reports of increases up to 25 percent (Breslin and Anderson 1996).

1.3 Objectives

The main objective of this research is to conduct an investigation allowing for a direct, experimental comparison between biological and engineering propulsion systems. For this study, an underwater vehicle was designed with the capability to produce either a steady or an unsteady jet for propulsion, akin to a squid and jellyfish, while utilizing the same η_{mech}. Given that the system has the same η_{mech} for both modes of propulsion, the η_{prop} is related to the η_o as $\eta_o = C \times \eta_{prop}$, where the constant $C = \eta_{mech}$. This results leads to an accurate comparison of the system's total efficiency for both modes of propulsion. In other words, measuring and comparing the propulsive efficiency for both modes of propulsion is equivalent to conducting a comparison of the total efficiency. A second objective of the research is to demonstrate that it is sufficient but not necessary to mimic the geometry and kinematics of swimming animals to replicate their propulsive performance. Using the conventional method of propulsion of a propeller platform can be similarly effective provided that the vehicle is capable of producing similar wake dynamics as those of swimming animals. The last objective serves to gain an understanding of the wake dynamics responsible for the production of increased propulsive performance. How does additional impulse generation due to two classes of ambient fluid entrainment in vortex ring formation play a role in altering the propulsive performance in pulsed jet propulsion?

1.4 Thesis Breakdown

This thesis is divided into five main chapters with a chapter for conclusions and 5 appendices of supporting material. Chapter 1 provides the background and support for the research. Chapter 2 describes the methodology behind the design of the vehicle and provides a detailed description of its construction and operation. Chapter 3 describes the experimental techniques and procedures used to characterize the jet flow and used in the investigation of the propulsive performance of the vehicle. Chapter 4 describes the characterization of the jet flow and the investigation of the propulsive performance of the vehicle by obtaining a measurement of the Froude efficiency and the total hydrodynamic efficiency. Chapter 5 provides insight into potential sources that contribute to increased propulsive performance. The analysis demonstrates that the acceleration of two classes of ambient fluid can lead to an increase in propulsive performance. A model is developed to investigate how the increase in total fluid impulse relates to the propulsive efficiency. Results are summarized and recommendations for future work are given in chapter 6.